

# Cell Permeability as a Parameter for Lead Generation in the Protein Tyrosine Kinase Inhibition Field

Christos Papageorgiou,\* Gian Camenisch and Xaver Borer

*Novartis Pharma AG, WSJ350.3.14, CH-4002 Basel, Switzerland*

Received 24 November 2000; accepted 29 December 2000

**Abstract**—Based on the inverse relationship between polar surface area and cell permeability and capitalizing on the properties of pyrrolopyrimidines **1** as protein tyrosine kinase inhibitors, pyrrolopyridones **2** were designed and synthesized as potential leads for the development of novel inhibitors with improved cell permeability properties. © 2001 Elsevier Science Ltd. All rights reserved.

Protein tyrosine kinases (PTKs) tightly regulate cellular function such as activation, proliferation, differentiation, and apoptosis and, therefore, represent attractive targets for the development of novel therapeutics, particularly in the fields of cancer, psoriasis, restenosis, or transplantation.<sup>1,2</sup> The huge majority of the structurally diverse enzyme inhibitors reported so far compete with adenosine triphosphate (ATP) for binding at the catalytic kinase domains, which share substantial structural similarities because of both the significant amino acid sequence homology and the conserved core architecture of most enzymes.<sup>3,4</sup> The claims on the availability of various potent and selective ATP-competitive inhibitors are usually based on data indicating the preferred inhibition of the enzymatic activity of the target kinase over that of a panel of control kinases in cell-free assays. Such selectivity data are independent of the cell permeation properties of the compounds and, therefore, of limited relevance for intracellular targets like PTKs because of the lack of a direct correlation between the efficacious concentration of compounds in a cell-free and cellular biological systems. This issue is even more important for PTK inhibitors as compared to inhibitors of other intracellular targets since, due to the elevated intracellular ATP concentration (1–5 mM), only substances with good cellular uptake and high intracellular potency can be expected to effectively bind the ATP-binding site.<sup>5</sup> Consequently, predictions on the potential of PTK inhibitors for adverse effects are difficult to make based on selectivity data generated without taking

into account the cell permeation properties of the compounds. The risk of systemic toxicity resulting from their poor discrimination between the numerous PTKs in vivo is of concern for the long-term application of such compounds and often restricts their field of application to life saving indications.

These considerations taken together underline the inherent complexity associated with the development of PTK inhibitors and reflect the interdependency of selectivity and cell-permeability. Therefore, the chemical derivation of lead structures for achieving high potency and enzyme selectivity should be preferentially carried out with those devoid of cell permeability drawbacks. Among the various physicochemical parameters evaluated as predictors of cell membrane permeability and, hence, passive epithelial permeability, the polar part of the molecular surface area (PSA) was shown to best correlate with the experimentally determined membrane permeability.<sup>6–8</sup> The PSA value of a compound can be estimated by computational methods while, for the experimental determination of its permeability, the Caco-2 cell monolayer based system is the most commonly used predictive assay.<sup>9</sup>

Pyrrolo[2,3-*d*]pyrimidines (**1**) have been described as selective inhibitors of the highly homologous enzymes belonging to the Src kinase family as compared to the EGFR kinase, the substitution pattern of the aromatic rings serving as a handle for selectivity modulation.<sup>10–13</sup> Aiming at the discovery of scaffolds with reduced PSA as potential leads for the development of selective PTK inhibitors and capitalizing on the structure of **1**, pyrrolopyridones **2** were designed and their cell

\*Corresponding author. Tel.: +41-61-324-6188; fax: +41-61-324-3036; e-mail: christos.papageorgiou@pharma.novartis.com

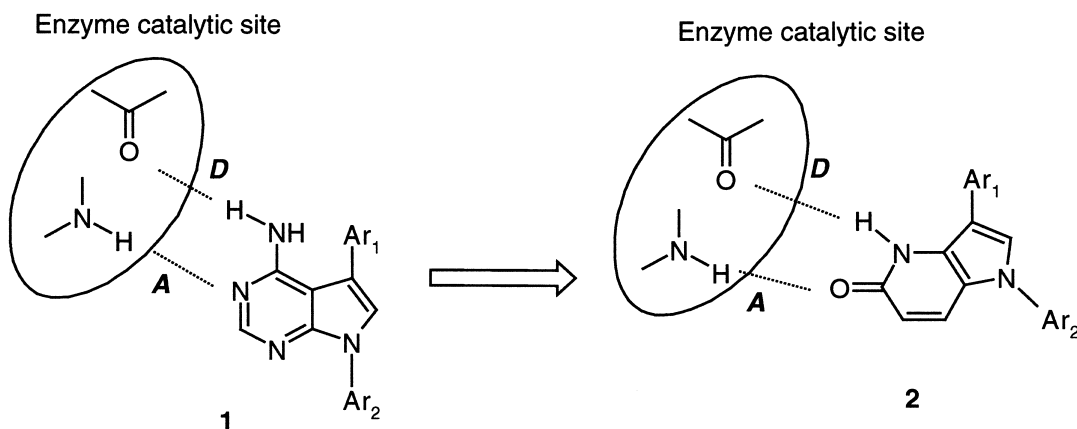


**Figure 1.** Generic structures and key hydrogen bonding characteristics of pyrrolopyrimidines **1** and pyrrolopyridones **2**.

membrane permeation aptitudes compared with those of the corresponding pyrrolopyrimidine derivatives. Care was taken to avoid large differences in the molecular weights of the compounds of the two substance classes and to integrate in **2** the key pharmacophore features necessary for compound-PTK recognition, namely a fused heterocycle containing a bidentate hydrogen bond donor-acceptor (D-A) motif (Fig. 1).<sup>10,13,14</sup> A comparative evaluation of the 3D PSA of **1a–c** and **2a–c** using their CORINA generate geometries and Connolly surfaces<sup>8</sup> indicated a better (mean 23%) cell permeation potential for the pyrrolopyridone derivatives (Table 1).

Aiming at the generation of the necessary lactam moiety in **2** from the corresponding 2-alkoxy pyridine, a readily cleavable protecting group was required that could be efficiently introduced into the commercially available 2-chloro-5-nitro-pyridine **3** at the beginning of the synthesis (Scheme 1). Preliminary investigations using

the methoxypyridine **4a** led to the azaindole **6a**<sup>15</sup> in good yields but could not be transformed into the corresponding pyridone due to the high stability of the methoxy group to the various demethylation protocols tried. Attracted by the successful use of the *tert*-butoxide moiety as a masking group for the generation of a pyrrolo[3,2-*b*]pyridone derivative, we subsequently aimed at the synthesis of the *tert*-butylpyridine **4b** but were unable to obtain this compound based on the reported procedure.<sup>16</sup> Finally, the trimethylsilylethanol reagent was found to be satisfactory for our purposes. Indeed, in the presence of *tert*-BuOK, it cleanly displaced chlorine in **3** affording **4c** in 65% yield.<sup>17</sup> The latter underwent a nucleophilic substitution of hydrogen upon treatment with the anion of 4-chlorophenoxyacetonitrile<sup>16</sup> to give **5c** (mp 74–76 °C), which was further cyclized into the corresponding azaindole **6c** (mp 121–122 °C) by catalytic hydrogenation in 76% yield. As a side product, the aniline corresponding to **5c** was isolated which could not be further transformed into **6c**. Iodination of the indole 3-position with *N*-iodosuccinimide afforded quantitatively **7** (mp 99–100 °C), the precursor for a Suzuki cross-coupling reaction. Using phenylboronic acid and *p*-methoxyphenylboronic acid, the 3-aryl azaindoles **8a** (oil) and **8b** (mp 117–118 °C) were obtained in 27 and 71% yield, respectively. The alkylation of the indole with benzylbromide and *p*-methoxybenzylbromide afforded **9a–c** which upon treatment with trifluoroacetic acid gave the desired pyridones **2a–c** as amorphous solids. No cleavage of the trimethylsilylethyl moiety took place in the presence of an excess of TBAF in various solvents. Evidence that **2a–c** adopted the lactam tautomeric form was obtained from their IR spectra which showed a strong absorption at 1634–1645 cm<sup>−1</sup> independent of the experimental conditions (KBr or CH<sub>2</sub>Cl<sub>2</sub> solution).

The computed polar surface area (PSA)<sup>8</sup> and the cell membrane permeability data (*P<sub>m</sub>*) determined in the human Caco-2 monolayer assay of compounds **1a–c**<sup>18</sup> and **2a–c** are summarized in Table 1.

In line with the reported findings,<sup>6–8</sup> an inverse relationship between calculated PSA values and *P<sub>m</sub>* was found; the smaller the PSA of a derivative the better it

**Table 1.** Calculated and experimentally determined cell penetration parameters

Compound	MW	3D PSA (Å <sup>2</sup> )	<i>P<sub>m</sub></i> <sup>a</sup> (10 <sup>−5</sup> cm/min)	Substrate affinity <sup>b</sup>
<b>1a</b>	300.4	46.6	ND	ND
<b>2a</b>	300.4	33.4	ND	ND
<b>1b</b>	330.4	58.2	78.2	Passive
<b>2b</b>	330.4	45.0	90.5	Passive
<b>1c</b>	360.4	69.2	61.9	Passive
<b>2c</b>	360.4	55.1	83.0	Passive

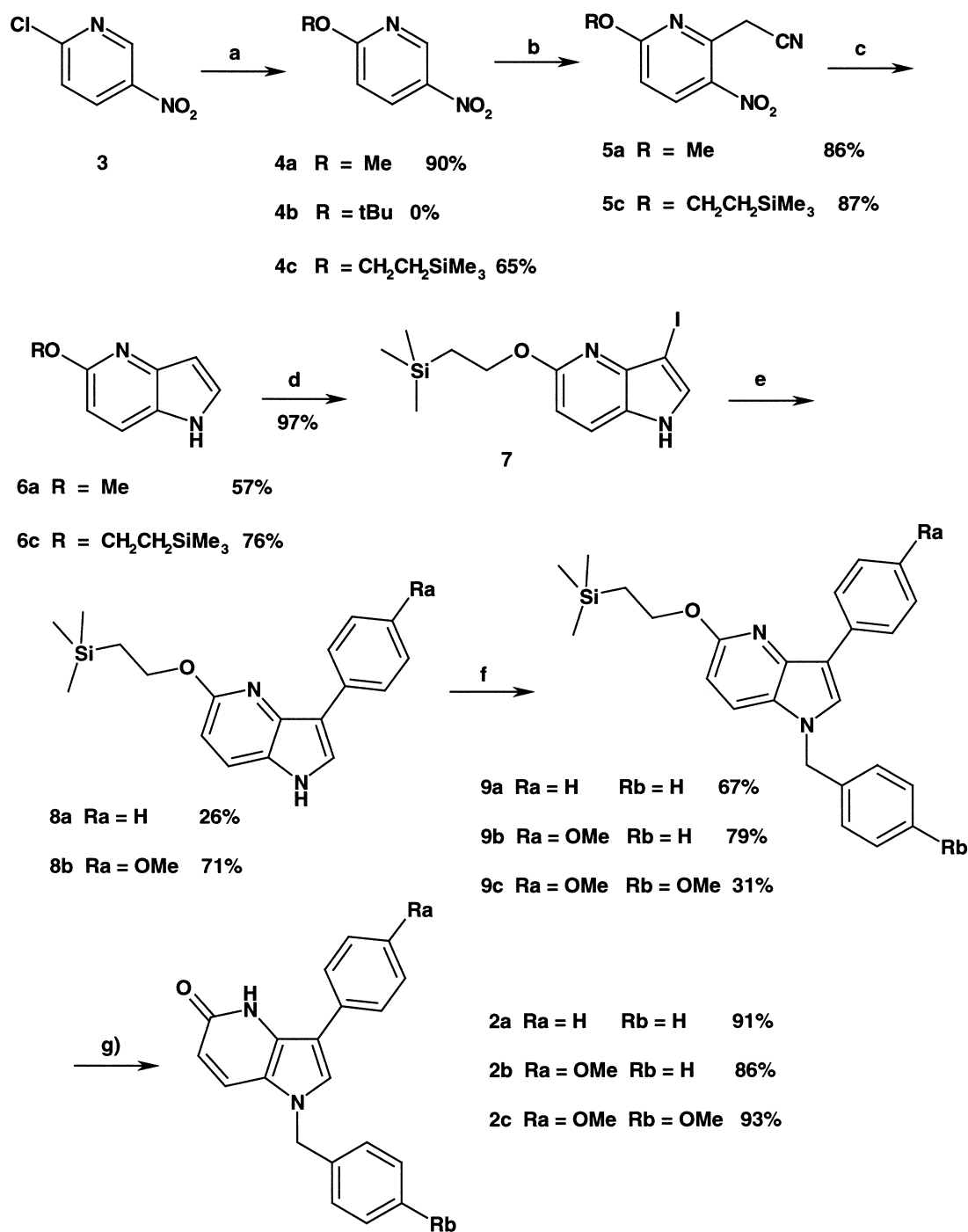
<sup>a</sup>Mean value of triplicates.

<sup>b</sup>Determined as the dependence of *P<sub>m</sub>* on the transport direction (i.e., similar or dissimilar rate of transport between apical-to-basolateral and basolateral-to-apical directions for the selected drug concentration). ND, not determined.

permeates the cell monolayer. Plotting of the PSA versus the  $P_m$  values obtained results in a linear, highly significant correlation with  $r^2=0.965$  (Fig. 2). Indeed, the 23% decrease in the PSA of **2b** over that of **1b** corresponds to a 15% improvement in the cell penetration of **2b** while the 20% difference between **2c** and **1c** leads to a 33% improvement for **2c**. No changes in the substrate specificities were found between **1b,c** and **2b,c**. Therefore, these results support the use of PSA as

predictor for the cell membrane penetration potential of a series of structurally and conformationally similar compounds and emphasize the overall contribution of cheminformatics in the drug-design field.

The consideration of the obtained structure–permeability data in the light of the selectivity–permeability issue in the PTK field indicates that pyrrolopyridones **2** can potentially be used for the development of selective



**Scheme 1.** Synthesis of pyrrolopyridones: (a) HOCH<sub>2</sub>CH<sub>2</sub>Si(CH<sub>3</sub>)<sub>3</sub> (1.0 equiv), *t*BuOK (1.3 equiv), DMF, rt; (b) *t*BuOK (2.2 equiv), 4-chlorophenoxyacetonitrile (1.1 equiv), THF, –10 °C, 3 h; (c) Pd/C, H<sub>2</sub>, EtOH (0.1 M); (d) NIS (1.1 equiv), THF, rt, 2 h; (e) PdCl<sub>2</sub>(dppf) (0.02 equiv), 2 N Na<sub>2</sub>CO<sub>3</sub> (3.0 equiv), ArB(OH)<sub>2</sub> (1.5 equiv), EtOH, reflux, 3 h; (f) NaH (1.1 equiv), ArCH<sub>2</sub>Br (1.5 equiv), THF, rt, 18 h; (g) CF<sub>3</sub>COOH (excess), 0 °C, 30 min.

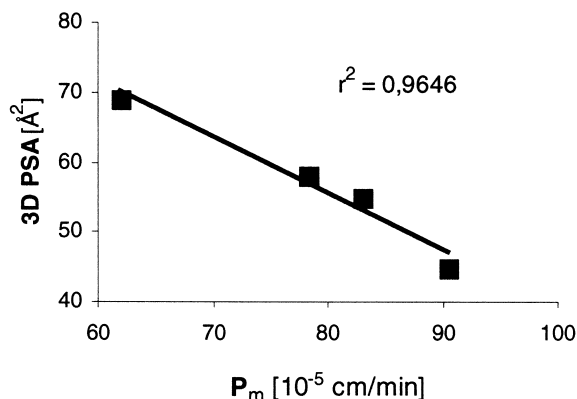


Figure 2. Correlation between 3D PSA and  $P_m$  data.

inhibitors that would allow probing the precise cellular function of a target enzyme and lead to safe therapeutic agents.

#### Acknowledgements

The authors thank Drs. Karl-Heinz Altmann and Eva Altmann for samples of **1a–c**.

#### References and Notes

1. Levitzki, A. *Pharmacol. Ther.* **1999**, *82*, 231.
2. Strawn, L. M.; Shawver, L. K. *Expert Opin. Invest. Drugs* **1998**, *7*, 553.

3. Al-Obeidi, F. A.; Wu, J. J.; Lam, K. S. *Biopolymers* **1998**, *47*, 197.
4. Traxler, P.; Furet, P. *Pharmacol. Ther.* **1999**, *82*, 195.
5. Lawrence, D. S.; Niu, J. *Pharmacol. Ther.* **1998**, *77*, 81.
6. van de Waterbeemd, H.; Camenisch, G.; Folkers, G.; Raevsky, O. A. *Quant. Struct.–Act. Relat.* **1996**, *15*, 480.
7. Palm, K.; Luthman, K.; Ungell, A.-L.; Straundlund, G.; Beigi, F.; Lundahl, P.; Artursson, P. *J. Med. Chem.* **1998**, *41*, 5382.
8. Ertl, P.; Rohde, B.; Selzer, P. *J. Med. Chem.* **2000**, *43*, 3714.
9. Artursson, P. *J. Pharm. Sci.* **1990**, *79*, 476.
10. Missbach, M.; Altmann, E.; Widler, L.; Susa, M.; Buchdunger, E.; Mett, H.; Meyer, T.; Green, J. *Bioorg. Med. Chem. Lett.* **2000**, *10*, 945.
11. Showalter, H. D. H.; Kraker, A. J. *Pharmacol. Ther.* **1997**, *76*, 55.
12. Traxler, P.; Furet, P.; Mett, H.; Buchdunger, E.; Meyer, T.; Lydon, N. *J. Med. Chem.* **1996**, *38*, 2285.
13. Traxler, P.; Green, J.; Mett, H.; Sequin, U.; Furet, P. *J. Med. Chem.* **1999**, *42*, 1018.
14. Zhu, X.; Kim, J. L.; Newcomb, J. R.; Rose, P. E.; Stover, D. R.; Toledo, L. M.; Zhao, H.; Morgenstern, K. A. *Structure* **1999**, *7*, 651.
15. Macor, J. E.; Newman, M. E. *Heterocycles* **1990**, *37*, 805.
16. Macor, J. E.; Burkhart, C. A.; Heym, J. H.; Ives, J. L.; Lebel, L. A.; Newman, M. E.; Nielsen, J. A.; Ryan, K.; Schulz, D. W. *J. Med. Chem.* **1990**, *33*, 2087.
17. Roberts, D. A.; Pearce, R. J.; Bradbury, R. H. *Eur. Pat. Appl.* 487252, 1992; *Chem. Abstr. Regno* 135900-24-2.
18. Widler, L.; Green, J.; Missbach, M.; Susa, M.; Altmann, E. *Bioorg. Med. Chem. Lett.* submitted for publication. For synthetic entries in the pyrrolo[2,3-*d*]pyrimidine class, see refs 10–13.